NEW APPROACH FOR FAST NUMERICAL PREDICTION OF RESIDUAL STRESS AND DISTORTION OF AM PARTS FROM STEELS WITH PHASE TRANSFORMATIONS

M. SCHÄNZEL*, A. ILIN* and V. PLOSHIKHIN**

*Corporate Sector Research and Advance Engineering Robert Bosch GmbH, 71272 Renningen, Germany, michael.schaenzel@de.bosch.com
**Airbus endowed chair for Integrative Simulation and Engineering of Materials and Processes University of Bremen, 28359 Bremen, Germany

DOI 10.3217/978-3-85125-615-4-54

ABSTRACT

Selective Laser Melting (SLM) is a promising additive manufacturing technology for production of complex and highly individual parts on short lead time request. Pre-processing assisted by numerical simulation can reduce defects which occur during construction and manufacturing and hence increase the quality of the parts and the efficiency of this technology. Especially the inherent strain method [1] is common and well suited for the fast numerical prediction and optimization of residual stresses and distortion of AM-parts. A major disadvantage of this method is the restriction to austenitic steels without phase transformations in the solid state during the process. The inherent strain method has only a limited validity for martensitic steels because the effects of phase transformations are not taken into account. However, an increasing number of materials to be processed requires a detailed numerical forecast also for martensitic steels to guarantee high quality parts.
This research work introduces an extension of the inherent strain method for the consideration of martensitic phase transformations during SLM-process. A multiscale approach, based on a coupled nonlinear thermo-mechanical finite element analysis and the further development of the inherent strain method combined with a new calibration procedure is proposed. It is demonstrated, that the developed approach can be effectively used for the forecast of structure distortions. The presented approach opens the way for the optimization of the additive manufacturing technology towards a defect-free manufacturing process.

Keywords: Selective laser melting, residual stresses, finite element analysis, phase transformation

INTRODUCTION

The economical production of highly individual products and complex parts requires innovative manufacturing technologies like the selective laser melting. This layer-based additive manufacturing technology becomes more common and relevant in various industrial branches like aerospace and automotive industries. Especially for these industries

with growing fields of application a clear understanding of the process is crucial to achieve a high process stability and reproducibility. In this case the numerical simulation can be used to develop a deeper understanding of the process.

For the beneficial application of the simulation in the production and development work efficient models with less calculation effort but nevertheless high accuracy are essential. In the area of selective laser melting especially the so called inherent strain method is a powerful tool for the fast prediction of distortion [1-2], residual stress as well as the cracking occurrence [3].

The method is based on the observations of Ueda [4-6] that the characteristic distribution of the permanent strains occurring in the weld area is directly related to the residual stresses. Ueda used an elastic analysis in which the occurring permanent strains are replaced by equivalent distributed loads to predict the residual stress. The method was successfully applied to large welding structures [7-12]. In Ref. [13] the so called 'Mechanical Process Equivalent' method is introduced for the determination of large structure distortions after welding process. As a further development this technique has been adapted for the selective laser melting [1-2] for the realization of the fast prediction of distortion and residual stress in AM parts using the finite element analysis.

However, the current state of the art of the inherent strain method in the case of SLM has been developed for stainless steels without phase transformations. If phase transformations occur in the process, the material behavior and condition of residual stress and strain can change entirely. This fact is shown in Fig. 1 with two standard cantilever beam specimen build-ups with equal process parameters but different materials. The cantilever built from austenite steel 1.4404 (AISI 316L) shows an upward distortion after the process and cutting off the supports while the one from martensitic steel 1.4057 (AISI 431) shows a downward distortion. This material behaviour cannot be modelled numerically with the current inherent strain method, which makes simulation-supported pre-processing of the SLM process difficult.

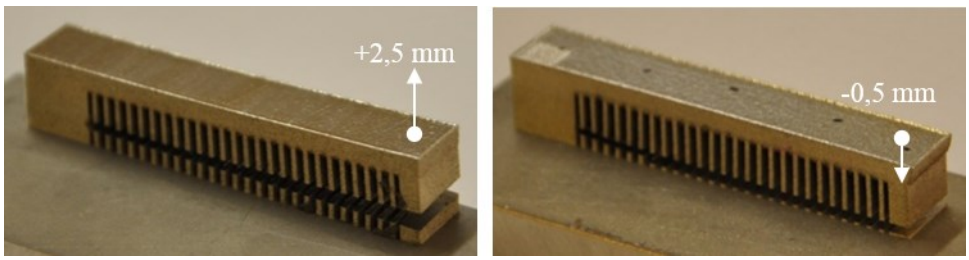

Fig. 1 Distorted cantilever of austenitic steel 1.4404 (left) and martensitic steel 1.4057 (right) built with same process parameters

A new approach of the inherent strain method for the consideration of the phase transformation related influence on the material behaviour is presented in this research work. The advanced inherent strain method allows the prediction of process related residual stresses and distortion even for martensitic steels.

Fundamental knowledge about the effects of phase transformation has been gained based on a non-linear thermo-mechanical macroscale FEM simulation, including a phase transformations model, in combination with high temperature experiments. A fast

calibration procedure is introduced for the new model with higher complexity. Validation with experiments at different temperatures confirms the advanced method.

NON-LINEAR MACRO SIMULATION MODEL

THERMO-MECHANICAL SIMULATION

The used sequentially coupled thermo-mechanical simulation model is based on the 'effective meshing' and 'adaptive heat source' model in reference to [14]. For the thermal analysis a full three-dimensional model is used. The plane or area of interest in this model is sufficiently fine meshed. The dimensions of the Goldak heat source [15] changes its dimension adaptively in correlation to the mesh density. This enables a physically plausible thermal modelling of the full geometry with a realistic temperature profile in the area of interest with a minimized calculation effort. The coupled mechanical simulation consists of a plane stress model of the plane of interest. Fig. 2 visualize the thermal three- and the mechanical two-dimensional model with temperature load.

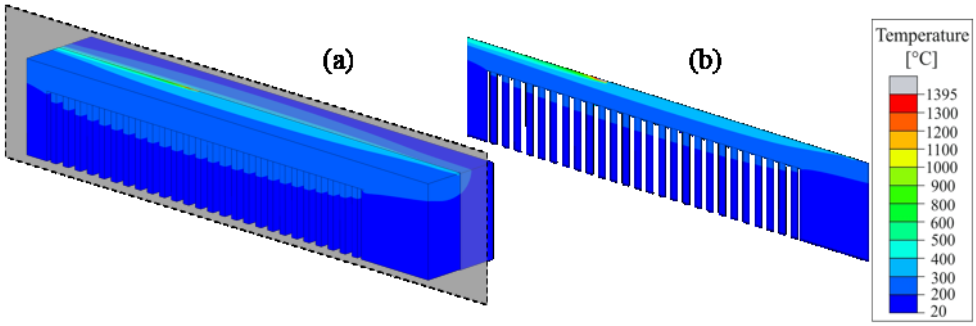

Fig. 2 Three-dimensional thermal (a) and two-dimensional mechanical model of the plane of interest (b)

The simulation of all scanning vectors as well as the intercooling during the coating process returns the realistic temperature profile and cooling rates. The information is essential for the calculation of the accurate mechanical behavior and is the input for the integrated phase transformation model. In the phase transformation model the austenitisation during the heating of the material is implemented as a linear transformation between the A_{c1} and A_{c3} temperatures, which are extracted from the TTT diagram and dilatometer experiments, see Fig. 3. In the cooling stage the transformation to martensitic phase begins at the martensitic start temperature M_s and is finished when reaching the finish temperature M_f. Between M_s and M_f the transformation is calculated based on the model of Koistinen and Marburger [16], see Eqn. (1). Variable V_γ represents the volume fraction of the retained austenite and T_q the cooling temperature reached during quenching. This formula neglects the cooling rate, which also can have an influence on the transformations.

Because of the high cooling rates in the SLM process this simplification appears reasonable, see cooling profile in Fig. 3.

$$V_\gamma = exp[-1.10 * 10^{-2}(M_s - T_q)] \quad (1)$$

To determine the phase transformation temperatures, dilatometer experiments are performed as well as calculations of material properties with the JMatPro [17] software. Based on this data the specific transformation temperatures are defined. In Fig. 4 are contrasted the experimental and JMatPro data with the simulation result of the numerical reproduction of the dilatometer experiment using the developed phase transformation model. The calculated proportions of the present phases were used in the mechanical material model to define phase-dependent material properties.

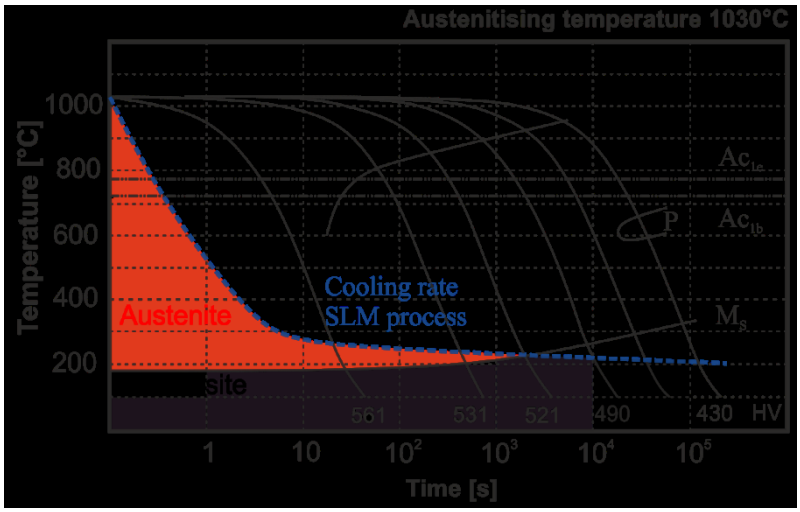

Fig. 3 TTT diagram of martensitic steel 1.4057 (AISI 431) [18] and cooling profile SLM process

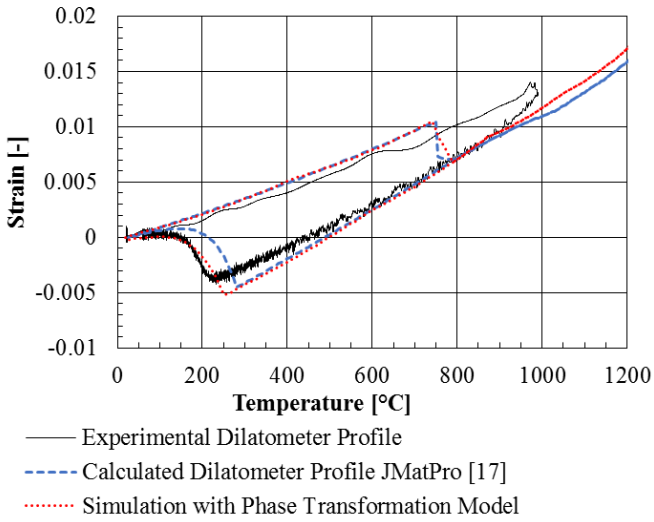

Fig. 4 Dilatometer experiment with 1.4057, calculated profile with JMatPro [17] and numerical reproduction with developed phase transformation model

RESULTS

The thermo-mechanical simulation has been used for a numerical reproduction of the cantilever build-up. The results of the calculated stress condition after the build-up are presented in Fig. 5. The numerical simulations are performed with the ABAQUS 2017 solver [19]. The austenite steel sample shows high deformation of the part after separating the support as a result of the tensile stresses on the top layers. The martensitic sample have only a low stress and distortion level.

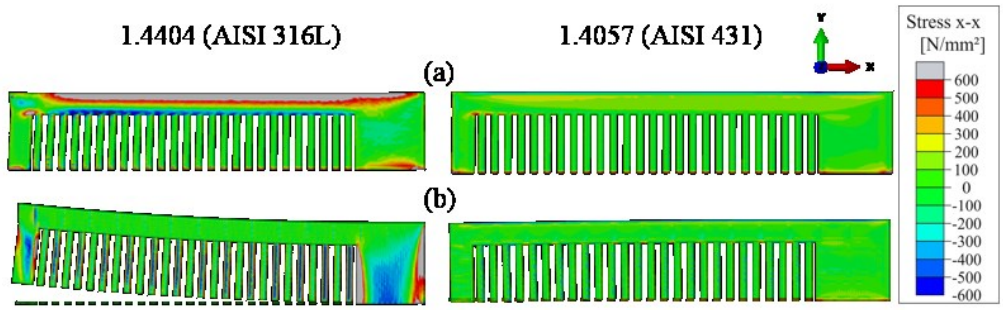

Fig. 5 Contour plot of residual stress after build-up (a) and with separated support structure (b)

For the validation of the model parameter settings with 350 W and 600 W laser power have been investigated. The experimental measured and the numerical calculated distortions are compared in Fig. 6. The results show a close correlation and a similar behaviour even for different parameters.

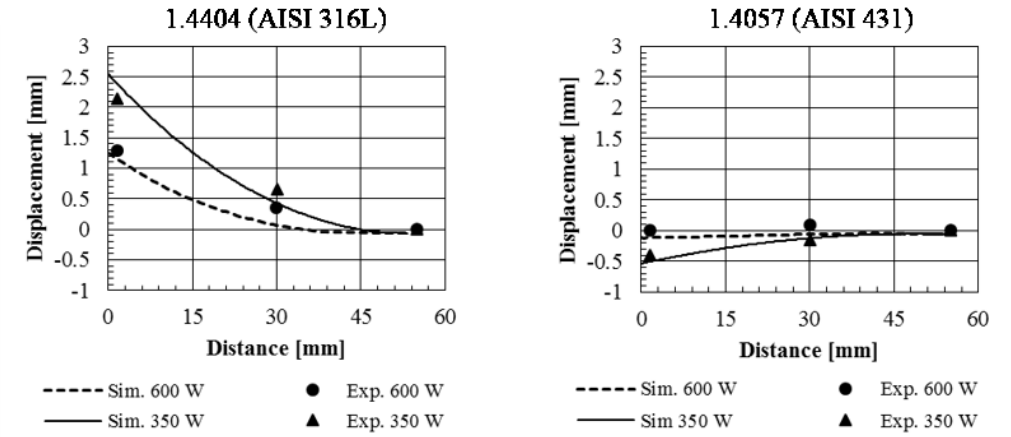

Fig. 6 Experimental and numerical results of the upward displacement of the cantilever specimen after separating the support structures

An explanation of the different distortion behaviour is presented in the calculation results of the phase transformation. In Fig. 7 are visualized the contour plots of the calculated phase states at the end of the heat transfer in the last layer. The 1.4404 steel is completely austenitic. Only the upper layer of 1.4057 is austenitic while the lower layers are martensitic. For the experimental build-up as well as the numerical reproduction the ground plate are heated to 200 °C. This temperature is almost reached during the intermediate cooling after every scanning step because of the high cooling rates. The martensite start temperature M_s of 1.4057 is quite above the pre-heating temperature of 200 °C, see Fig. 3. Consequently a layer wise transformation from austenitic to martensitic phase after each layer takes place for the martensitic steel.

There is a change of the face-centered cubic crystal structure to the body-centered tetragonal crystal structure during the transformation from austenitic to martensitic phase. The phase transformation results in an increase of the volume, like the dilatometer profiles in Fig. 4 visualizes. As a result the 1.4057 steel shows a compensation of the thermal shrinkage by the layer-wise phase transformation and the accompanied increase of the volume. The austenitic 1.4404 steel does not have this compensation effect which is why thermal shrinkage leads to the high tensile stresses and high distortion.

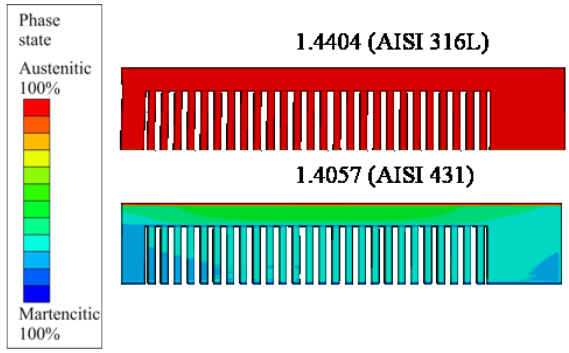

Fig. 7 Volume fractions of austenite and martensite after scanning

As a conclusion the stress and strain condition of martensitic steels after build-up is strongly influenced by the phase transformation. The shrinkage strain of the material can be fully compensated if the process is characterized by a layer-wise transformation back from austenite to martensite. Numerical simulations of the build-up with a heating temperature of 300 °C during the process show an increased distortion of the 1.4057, similar to the 1.4404 material. In this case the M_s temperature and pre-heating temperature are almost identical. The transformation takes place in deeper layers or the whole part remains in austenitic phase until the process is completely finished. The missing layer-wise compensation of the shrinkage results in significant higher distortions.

EXPERIMENTAL WORK

HIGH-TEMPERATURE TESTING

For the investigation of the layer-wise shrinkage compensation thesis different cantilever build-ups were performed with another martensitic chrome steel. It is intended to evaluate if a high temperature influences the transformations and thus the distortion. This steel has a temperature interval for phase transformation between 200 °C and 300 °C. Because a high temperature build-up is quite costly, the preliminary studies were performed with standard SLM Solution 280 HL system with a 200 °C heating system. To reach higher temperatures the part is built on thin support walls to disturb heat dissipation and force an overheating of the component, see Fig. 8. When looking at the surfaces of the components, different surface colors becomes visible. The overheated sample looks dark discolored like an overhanging area. It could not be clarified directly whether these are tempering effects, but the color is a direct indicator for high process temperatures as the later performed high temperature build-ups show.

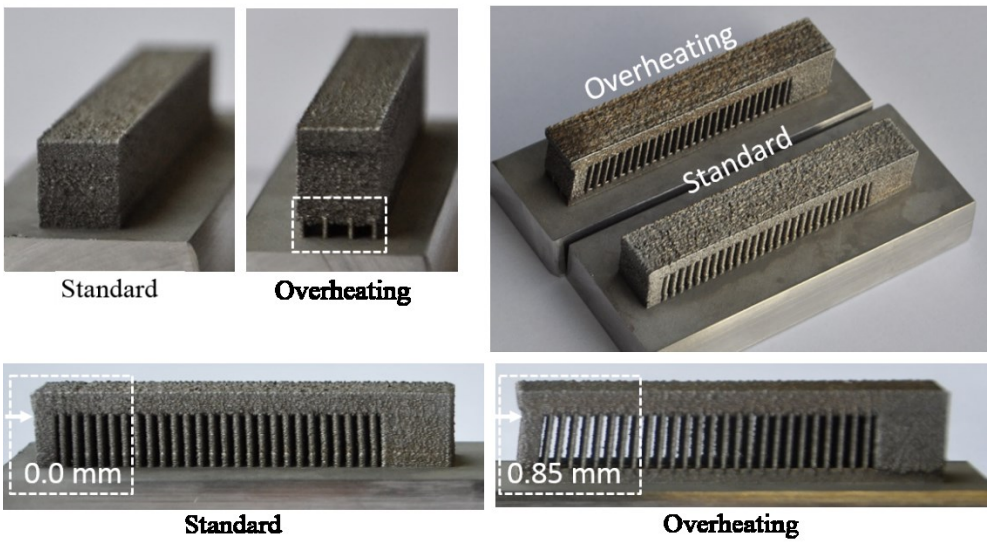

Fig. 8 Cantilever specimen made of martensitic chrome steel. Different support structures were used to enforce heat accumulation due to disturbed heat conduction

Remarkable is the different distortion level of the samples. Even though the same material and parameters are used, the overheated sample shows a significant higher distortion. It is assumed that the degradation of the heat conduction leads to a heat accumulation of the sample almost above 300 °C and therefore above M_s temperature. The higher process temperatures prevent a layer-wise transformation as the standard sample indicates. As a result the overheated sample shows high distortion due to the not compensated shrinkage. Fig. 9 visualizes the measured upward displacement after separating the supports. Deviation of the distortion behavior can be observed.

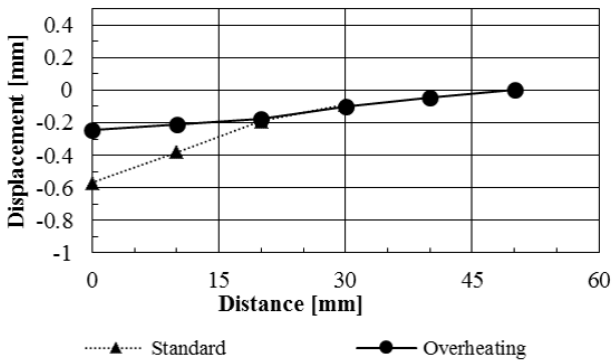

Fig. 9 Measured upward displacement of the martensitic chrome steel cantilever samples

In order to compare the observed behaviour to the 1.4057 martensitic steel, further tests are performed with a SLM Solution 280 HL machine with a heating system until 650 °C. Samples are built with same parameters at pre-heating temperatures of 150 °C, 350 °C, 450 °C and 650 °C, see Fig. 10.

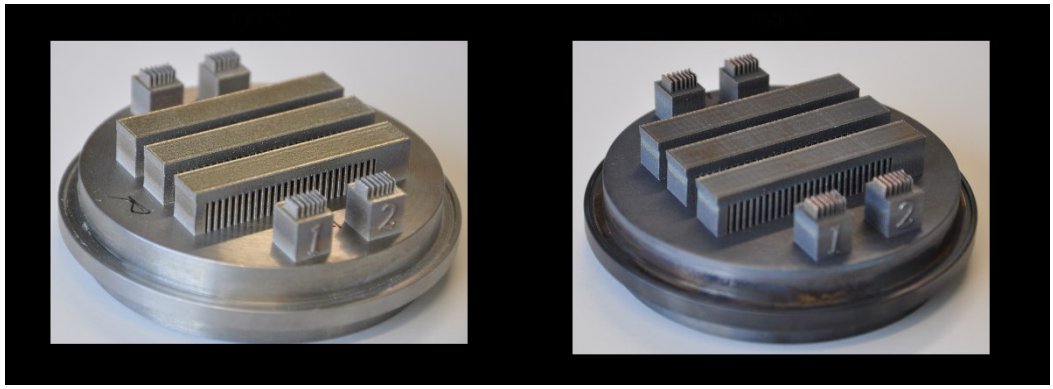

Fig. 10 Cantilever specimen of 1.4057 built with different pre-heating temperatures and different colored surfaces

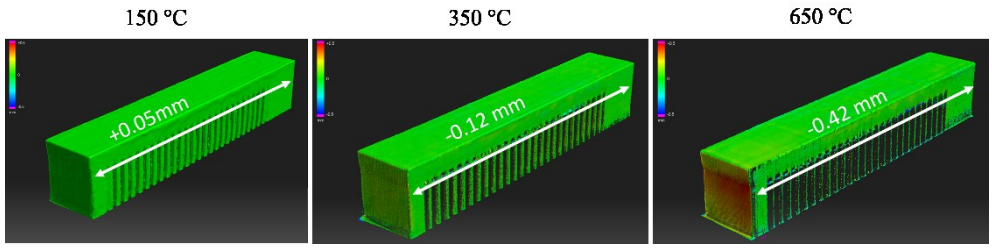

Fig. 11 3D-scanning results of cantilever specimen of 1.4057 with color map of the deviation to the reference geometry for different pre-heating temperatures

A three-dimensional scanning system is used for measuring and visualization of the distortion level, shown in Fig. 11. The 150 °C sample reveals a minimum distortion. With an increase of the temperature an increase of the shrinkage can be observed: The measurements of the longitudinal and upward displacement is represented in Fig. 12.

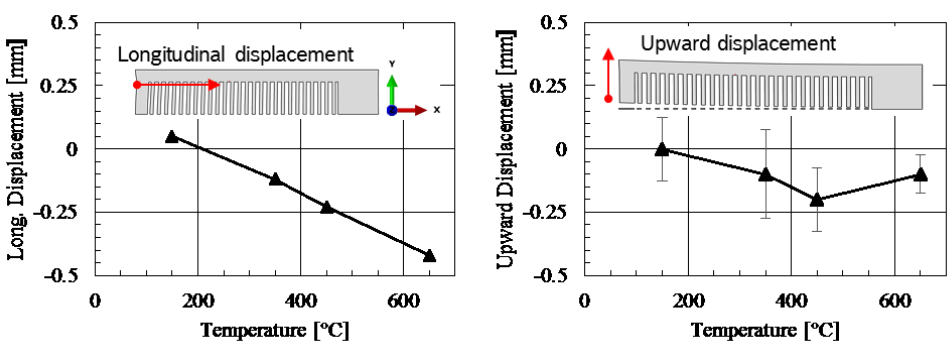

Fig. 12 Distortion measurements of 1.4057 samples for different pre-heating temperatures

HIGH-TEMPERATURE MATERIAL BEHAVIOUR

For a clear understanding of the material behavior of the martensitic steel 1.4057 next to the dilatometer experiments, tensile test at different temperature are performed on Gleeble machine [20], see Fig. 13. The specimens are pre-heated to 1350 °C close to solidus temperature for the complete austenitization. During cooling, the temperature is held at the respective temperature level and the tensile test is performed. The results show a significant decreased flow stress even at 200 °C. For the components these results indicate a significant reduction of the high stress peaks in the process caused by plastic deformation. Furthermore the events in lower temperatures ranges are of significant importance. That clarifies the influence of the phase transformation which occur in exactly this range.

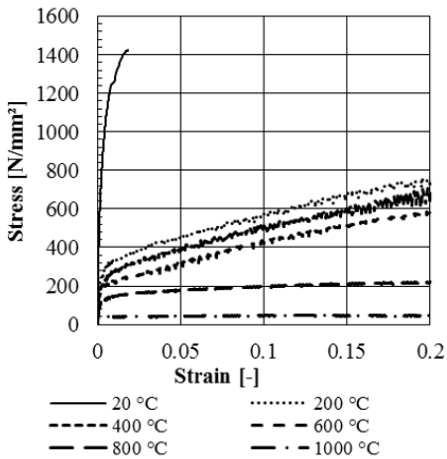

Fig. 13 Temperature dependent stress-strain properties of 1.4057 martensitic steel

DISCUSSION

The experimental investigation with the cantilevers build-ups using different process temperatures confirms the thesis based on the macro simulation result. Higher temperature lead to a reduced effect of the layer-wise shrinkage compensation. It is assumed that the increased pre-heating temperature in combination with the heat accumulation caused by the laser power prevent the material from cooling down. The upper layers stay above M_s temperature and therefore in austenite phase. The transformation back to martensitic phase occurs later in the process with a layer delay. It is assumed that there is a dependency of the layer delay of the transformation to the process parameter as well as the pre-heating temperature. On average, the layer delay for the entire component is expected to remain constant if the heat transfer to the base plate is reasonably good due to sufficient amount of support structures.

NEW APPROACH FOR FAST SIMULATION CONSIDERING PHASE TRANSFORMATION

STATE OF THE SCIENCE

The new approach presented in this research work is based on the mechanical static FEM process model for the fast estimation of residual stresses and strains, also known as inherent strain method, introduced by [1-2].

A layer-wise finite element model is used to apply the inherent strain method on the additive manufacturing process. The build-up process is modeled by a layer-wise adding of the elements and the applying of the inherent strain tensor. The load of the strain tensor is modeled as a volume strain boundary condition. The simulation is performed at room temperature. The inherent strain tensor ε^{inh} represents the material condition in terms of the remaining plastic strain caused by the solidification and shrinkage process and is defined after Eqn. (2). In Eqn. (2), ε^{t} denotes the total strain, ε^{E} the elastic strain, ε^{pl} the plastic strain, ε^{pt} and ε^{cr} the transformation and creep strain. For simplification it is assumed, that after the process the thermal strain is equal to zero as well as the creep strain. In the current state of the science method also the transformation strain is neglected and set to zero, that finally the inherent strains ε^{inh} are the remaining plastic strains.

$$\varepsilon^{inh} = \begin{pmatrix} \varepsilon_{xx} \\ \varepsilon_{yy} \\ \varepsilon_{zz} \\ \varepsilon_{xy} \\ \varepsilon_{yz} \\ \varepsilon_{zx} \end{pmatrix} = \varepsilon^{t} - \varepsilon^{E} = \varepsilon^{the} + \varepsilon^{pl} + \varepsilon^{pt} + \varepsilon^{cr} = \varepsilon^{pl} \tag{2}$$

The strain tensor ε^{inh} can be calibrated for the specific process parameters of the build-up to be investigated. The calibration of the tensor is performed by the iterative comparison between the displacement of an experimental built standard cantilever beam and the calculated displacement by the numerical reproduction. The results of the inherent strain method show to some extent a dependency on the layer thickness and mesh, as well as the assigned strain and material [2]. An overview of the method is shown in Table 1.

Table 1 Overview of the state of the science inherent strain method

Load application	Standard case	Applied material properties
Layer wise	$\varepsilon^{inh} = \begin{pmatrix} \boldsymbol{\varepsilon_x} \\ \boldsymbol{\varepsilon_y} \\ \boldsymbol{\varepsilon_z} \end{pmatrix} = \boldsymbol{\varepsilon^{scan}}\ (T_L \rightarrow T_{Rt})$ *to be calibrated*	Room temperature T_{Rt}

The main disadvantage of the state of the science inherent strain method is not considering the phase transformation strain ε^{pt}. Also the applied temperature is not taken into account which can lead to larger deviations at high temperatures. Therefore the method is only valid for austenitic steels and the applicability for martensitic steels is not given.

NEW APPROACH

To ensure a reliable numerical prediction of the distortions for martensitic steels the phase transformation strain ε^{pt} have to be considered. The results of the thermo-mechanical simulation demonstrated the temporal occurrence of the phase transformation as the major influence on the mechanical behaviour. Even at pre-heating temperatures above M_s temperature a delayed transformation could be observed where only austenitic structure should be present. It is assumed that the heat convection with inert gas on the top surface and the heat conduction to the powder prevent a constant pre-heating temperature in the entire part and cause temperatures below pre-heating temperature. Hence, the process can be divided into three different cases in dependency of the pre-heating temperature, see Fig. 14. Case one represents a layer wise transformation for a pre-heating temperature that is significantly lower than the M_s temperature. In the second case, the heat accumulation supported by higher pre-heating temperature leads to a layer delay *dn* of the martensitic transformation. The third case is characterized by temperature field significant above the M_s temperature throughout the entire process as a result of a high pre-heating temperature. In this case, the phase transformation took place only at the end of the process during the final cooling of the component.

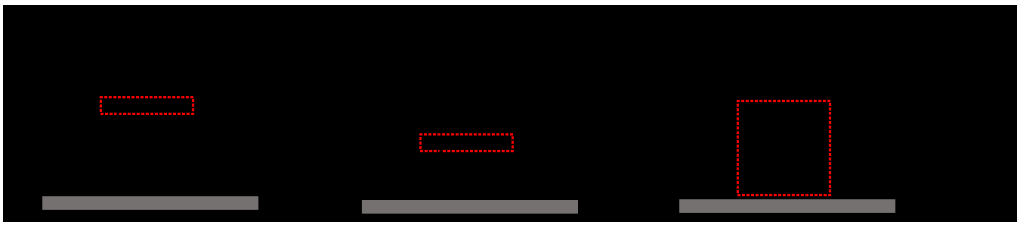

Fig. 14 Different cases for the sequence of phase transformation during the process in martensitic steels

In a first model the inherent strain method has been extended by the additional phase transformation strain tensor ε^{pt}. The tensor ε^{pt} represents the increasing of the volume caused by the change of the lattice structure and is based on the dilatometer experiments, defined in Eqn. 3.

$$\varepsilon^{pt} = \begin{pmatrix} \varepsilon_x^{pt} \\ \varepsilon_y^{pt} \\ \varepsilon_z^{pt} \end{pmatrix} = 0.00325 \tag{3}$$

The application of the strain tensor ε^{pt} is taken place with a layer delay *dn* in parallel to the application of the standard inherent strain tensor ε^{inh} in the current layer. A numerical series of tests were performed with a setup of $\varepsilon^{inh} = -0.003$ and a variation of the layer delay *dn* from 0 to 6. The results are shown in Fig. 15. The analysis shows that although the total amount of the applied strain is zero and both strains have the same size, the distortion can vary widely in dependency of the delay *dn.* Significant variables that characterize the process are the distortions in longitudinal direction before separating the support and the upward distortion after as already stated in the experimental investigations.

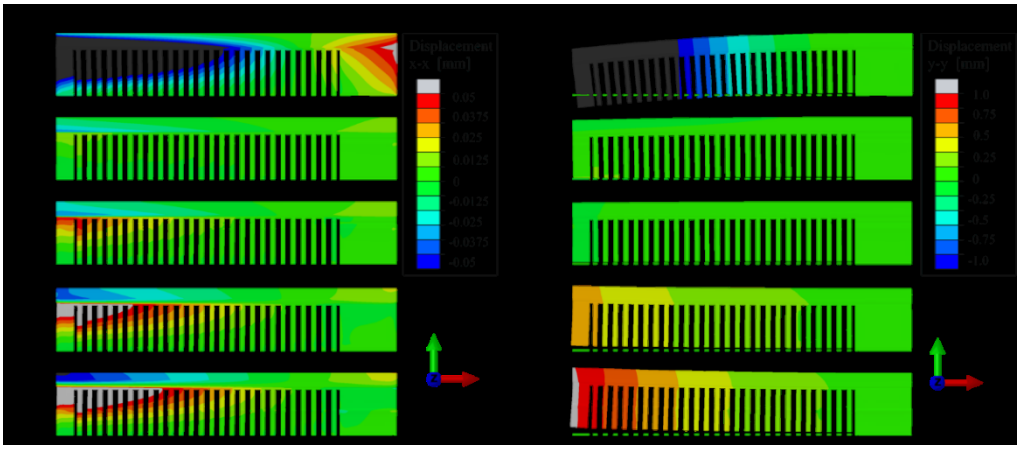

Fig. 15 Numerical analysis of an extended inherent strain method with regard to a layer delayed volume increase due to martensitic phase transformation. Contour plots of distortion in x-direction before separating support (left) and distortion in y-direction after (right)

The numerical analysis was performed with the use of room temperature material properties. Exceeds the delay *dn* five layers, an upward displacement could be found. Because this is contrary to the experimental result is assumed that the high yield stress at room temperature prevent a plastic deformation of the material and thus the reduction of stress peaks. As a consequence, temperature-dependent flow curves are introduced in the model.

For another improvement of the quality of the results the strain tensor ε^{inh} is divided into different strain tensors ε^{scan} and ε^{cool}. The tensor ε^{scan} represents the layer-wise shrinkage due to the intermediate cooling from solidification temperature T_L to pre-heating temperature T_{Bt}. The tensor ε^{cool} denotes the shrinkage strain caused by the final cooling from pre-heating temperature to room temperature T_{Rt}.

Table 2 shows an overview of the final developed simulation procedure with three calculation steps. It is also listed which temperature the material properties are applied in the respective step.

Table 2 Overview of the new approach of the inherent strain method for martensitic steels

Load application	New Approach	Applied material properties
Layer wise	Step 1: $\boldsymbol{\varepsilon^{scan}}$ $(\mathrm{T_L} \rightarrow \mathrm{T_{Bt}}) = \begin{pmatrix} \boldsymbol{\varepsilon_x} \\ \boldsymbol{\varepsilon_y} \\ \boldsymbol{\varepsilon_z} \end{pmatrix}$ *to be calibrated*	Pre-heating temperature $\mathrm{T_{Bt}}$
With layer delay $(\boldsymbol{dn})$ *to be calibrated*	Step 2: $\boldsymbol{\varepsilon^{pt}}$ *to be calculated/ measured*	Pre-heating temperature $\mathrm{T_{Bt}}$
Post process	Step 3: $\mathrm{T_{Bt}} > \mathrm{T_{Mf}}$: $\boldsymbol{\varepsilon^{cool1}}$ $(\mathrm{T_{Pt}} \rightarrow \mathrm{T_{Rt}})$ $\mathrm{T_{Bt}} < \mathrm{T_{Mf}}$: $\boldsymbol{\varepsilon^{cool2}}$ $(\mathrm{T_{Bt}} \rightarrow \mathrm{T_{Rt}})$ *to be calculated*	Room temperature $\mathrm{T_{Rt}}$

The application of the new approach requires the following parameters to be known: The strain tensors ε^{scan}, ε^{pt} and ε^{cool} as well as the delay *dn*. Those parameters can be classified in ones which have to be calibrated and ones which can be calculate or measured. Dilatometer experiment or a numerical reproduction are used to determine ε^{pt}. A numerical Satoh test modelling [21] is used to calculate the post process shrinkage ε^{cool}, see Fig. 16. A further distinction is made here whether the pre-heating temperature is above or lower than the middle phase transformation temperature T_{Pt}.

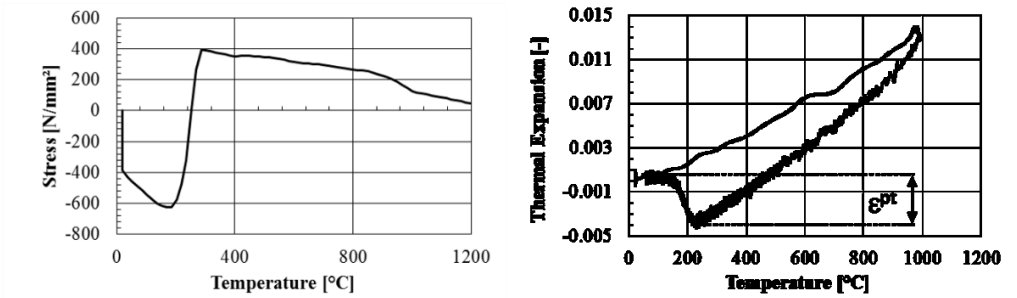

Fig. 16 Satoh test modelling for calculation of ε^{cool} and dilatometer curve to determine ε^{pt}

For the definition of the tensor ε^{scan} and the delay *dn* an iterative experimental calibration is used with a numerical reproduction in analogy to the state of the art method. In addition the longitudinal shrinkage $U_{X\text{-}X}$ is measured before separating the supports as a second input variable for the calibration, next to the upward displacement $U_{Y\text{-}Y}$, see Fig. 17. With the two input variables it is possible to determine the missing parameters iteratively.

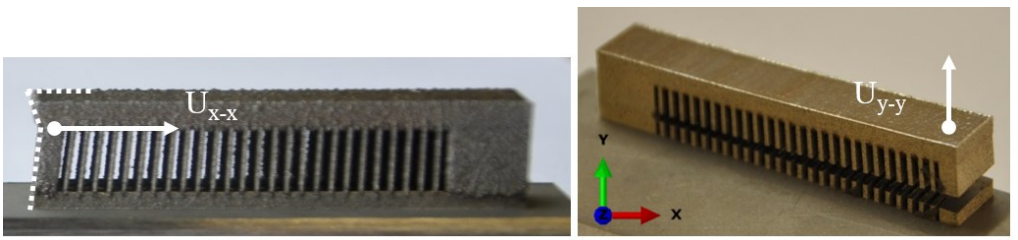

Fig. 17 Definition of calibration input variables: Longitudinal shrinkage $U_{X\text{-}X}$ (left) before separating and upward displacement $U_{Y\text{-}Y}$ (right) after separating the support structures

In order to reduce the manual calibration effort, which can already time consuming with two parameters, an automated calibration is implemented, see Fig. 18. The calibration procedure is structured in a pre-processing stage and a parameter calibration stage.

Fig. 18 Visualization of the calibration procedure of the model parameters

Optimization algorithms are used for the iteratively calibration to reduce the calculation effort. In Eqn. 4 is shown the optimization problem, which have to be minimized to find the best solution for the tensor ε^{scan} and the delay *dn* with the best agreement between simulation and experiment.

$$arg\,min\,f(\,\varepsilon^{inh\,scan}\,, dn) = arg\,min\,|U_{Exp} - U_{Sim}| \tag{4}$$

Investigations of the fitness landscape have shown that the optimization problem can be of high complexity and multiple local minima can exist. In order to find best solution and therefore the global minimum, it is proposed to use hybrid optimization algorithm. Those optimization algorithm use a combined search existing of an “exploration” and “exploitation” part. In a first step is fulfilled a global search to explore the solution area. In a following step the promising optima is identified. In Fig. 19 is shown a contour plot of the fitness landscape for the optimization problem of the 150 °C pre-heating calibration with different local minima.

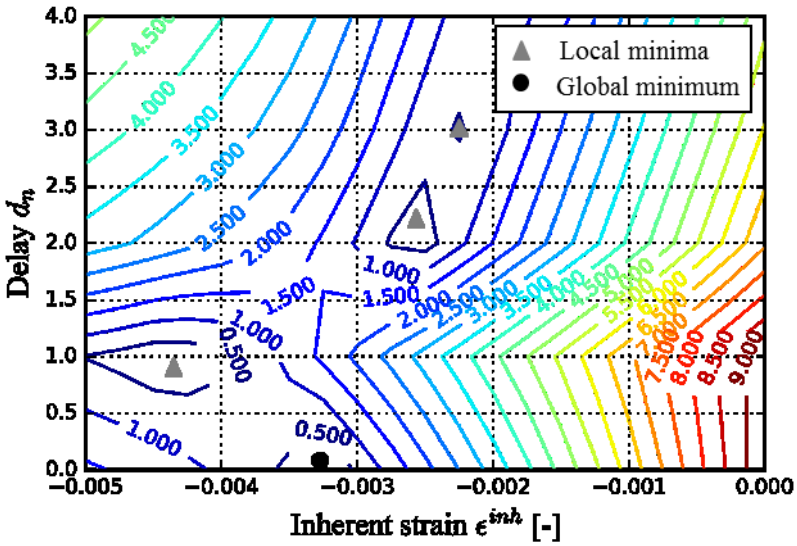

Fig. 19 Visualization of the fitness landscape $f(\varepsilon^{inh\,scan}, dn)$ with different local minima

SIMULATION RESULTS

In order to validate the developed approach over a wide temperature range, the cantilever build-ups at different pre-heating temperatures are repeated numerically. Table 3 lists the calibrated and applied parameters of the model for the different temperature levels. It can be stated that the strain tensor ε^{scan} decreases with an increasing temperature. This observation is reasonable because the temperature interval from solidification to construction temperature $T_L \rightarrow T_{Bt}$ is reduced relevant and therefore the shrinkage strain tensor ε^{scan}. The delay dn of the transformation increases with an increase of the pre-heating temperature. However, the calibration showed that even for the 650 °C sample the third case could not be determined, classified in Fig. 14 and characterized with a complete post process phase transformation. The calibration however confirmed the increase in delay for higher temperatures. Because of the absence of temperature monitoring systems, the surface temperature in the process could not be determined experimentally. It is assumed, that the pre-heating system was unable to maintain the desired pre-heating temperatures with an increase in height of the specimen.

Table 3 Overview of calibrated model parameters for different construction temperatures

Pre-heating **temperature**	**150°C**	**350°C**	**450°C**	**650°C**
ε^{scan}	-0.00325	-0.0032	-0.00315	-0.00315
layer delay (dn)	0	2	4	Post process
ε^{pt}	+0.00325	+0.00325	+0.00325	+0.00325
ε^{cool1}	-0.00148	-	-	-
ε^{cool2}	-	-0.001908	-0.001908	-0.001908

The results of the distortion $U_{X\text{-}X}$ and $U_{Y\text{-}Y}$ of the calibrated models are visualized as contour plots in Fig. 20. In comparison to the numerical analysis shown in Fig 15 even for higher transformation delays an upward displacement is not shown. These differences in behavior can mainly be attributed to the implemented temperature-dependent flow curves.

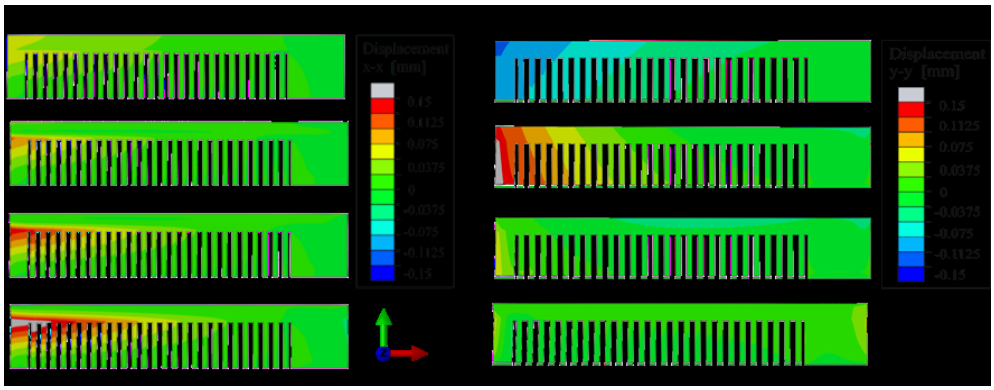

Fig. 20 Contour plots of numerical distortion calculation with calibrated model parameters in x-direction before separating support (left) and distortion in y-direction after (right)

Fig. 21 represents the comparison of the experimental and simulated results. The values confirm a close correlation of the experiment and the numerical model at low and mid temperature levels. Only for the 650 °C larger deviations can be determined. The proportion of longitudinal shrinkage in the experiment is higher than in the simulation. In this case it is assumed that the real process temperature is significantly below the pre-heating temperature set and the applied material properties are not realistic. However, the simulation shows the same tendency of an increasing longitudinal shrinkage with rising construction temperatures.

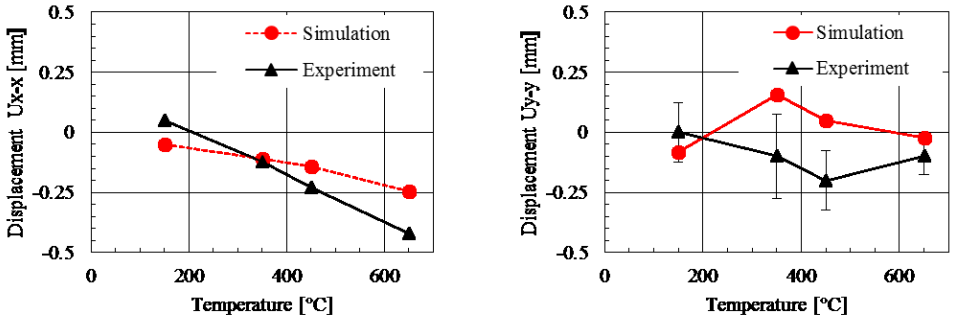

Fig. 21 Validation of calculated distortion using the new approach with measured distortion of the cantilever

DISCUSSION

The new developed approach allows for the first time the fast prediction of residual stresses and distortion for martensitic phase transformation steels. The results make clear that a calculation based on the state of the art inherent strain method is not suited for numerical calculation of accurate results for martensitic steels. However, the developed method is still a substitute model that does not represent all physical phenomena. The creep strain can have especially for high process times in combination with high temperatures a relevant influence. Because no temperature and temporal information is available the creep strain could not be considered. Despite the fact that no direct temperature information is available, temperature dependent material properties are introduced to take into account the reduced yield strength at high pre-heating temperatures. In this way the results could improve significantly. But this also increases the effort since the necessary properties have to be determined first.

The chronological sequence of the induced strains has proved to be significant for the quality of the results. This phenomenon should be considered by the segmentation of the standard shrinkage strain ε^{inh} into the two different strains ε^{scan} and ε^{cool}. During development of the presented method a subdivision in even more single shrinkage strains has been investigated. Especially a first layer-wise strain from solidification temperature to pre-heating temperature $\boldsymbol{\varepsilon_1^{inh}}\,(T_L \rightarrow T_{Bt})$, in combination with a second shrinkage strain from pre-heating temperature to the middle phase transformation temperature $\boldsymbol{\varepsilon_2^{inh}}(T_{BT} \rightarrow T_{Pt})$ applied layer delayed together with the transformation strain ε^{pt} and a third post process strain $\boldsymbol{\varepsilon_3^{inh}}(T_{PT} \rightarrow T_{Rt})$ was promising. Also this approach is based on two calibration parameters because the second strain $\boldsymbol{\varepsilon_2^{inh}}(T_{BT} \rightarrow T_{Pt})$ could be also calculated using a numerical Satoh test. However, the application of more strain tensors is prevented by the process temperature, because the current pre-heating systems are not able to maintain the adjusted pre-heating temperature within the entire specimen. Due to this uncertainty of the temperature, an even finer division is currently not useful for the current machines or without more detailed temperature information and is the restriction for the application of the developed model. The cantilever, which is used for the calibration, just reflects a standard condition with sufficient support structures and therefore an average heat

conduction. For a standard build-up such a condition with an average heat dissipation is intended, which distinguishes the cantilever to a representative sample. If the density of support structures varies widely, then as a consequence the heat dissipation and process temperature may also differs. In this case, a high-quality prediction is even more difficult because the phase transformation are generally initiated by the temperature.

The results confirm the importance of phase transformations for the mechanical behaviour of martensitic steels as already described in [14]. The investigation demonstrate that if the temperatures in the process kept below the middle phase transformation temperature the layer-wise shrinkage compensation enables an almost stress- and distortion-free component. The use of higher construction temperatures therefore should be reconsidered for the martensitic steels.

SUMMARY AND OUTLOOK

In this research work a new method for the fast numerical prediction of process related residual stresses and distortion for martensitic phase transformation steels in selective laser melting is presented. The approach is based on the inherent strain method, which is further improved by the findings of a performed detailed coupled thermo-mechanical analysis and high temperature experiments. The investigated experiments and simulation indicated the increase of the volume caused by the transformation of austenitic face-centered cubic crystal structure into the martensitic body-centered tetragonal grain structure as a mayor influence parameter on the mechanical behaviour of the component. Especially the delay of the phase transformation is of great importance and is considered in the model. Another important influencing factor is the time sequence of the applied strains. Therefor the standard inherent strain tensor is distributed into different shrinkage strains. For the further improvement of the quality of the results also for an increased pre-heating temperature-dependent flow curves are introduced in the material model. The newly developed model was extended by one parameter to be calibrated, compared to the standard inherent strain method. Therefore, in addition to the upward deformation, the longitudinal shrinkage before the supports were cut off was introduced as an additional calibration input parameter.

For the following investigations the development of a new specimen for the characterization of the temperature condition in the component is planned. The thermally introduced phase transformation strains at M_s temperature could be used to analyse the process and machine specific temperature profile across the depths of the component. The presented approach is based on the assumption of a geometry-independent homogeneous heat dissipation. Geometry related hot spots caused by a reduced heat conduction are not taken into account. A further development of the presented method therefor could be the coupling to a fast numerical thermal analysis of the component. Areas with increased heat accumulation could be detected and the time sequence of the applied strains could be further refined for an improvement of accuracy of the numerical prediction.

REFERENCES

[1] N. KELLER, V. PLOSHIKHIN: 'New method for fast predictions of residual stress and distortion of AM parts', *Solid Freeform Fabrication Symposium*, 2014.

[2] N. KELLER, J. SCHLASCHE, H. XU,V. PLOSHIKHIN: 'Simulation Aided Manufacturing: Scanning Strategies for Low Distortion in Laser Beam Melting Processes', *Fraunhofer Direct Digital Manufacturing Conference*, pp.3-6, 2016.

[3] M. SCHAENZEL, D. SHAKIROV, A. ILIN, V. PLOSHIKHIN: 'Development of a cracking criteria for the numerical failure prediction of support structures, *Fraunhofer Direct Digital Manufacturing Conference*, 2018.

[4] Y. UEDA, M.G. YUANG: 'Prediction of Welding Residual Stresses in T and I joints Using Inherent Strains. Report 3', *Welding International*, (6.4), pp.263-269, 1992.

[5] Y. UEDA, M.G. YUANG: 'Prediction of Residual Stresses in Butt Welded Plates Using Inherent Strains', *Journal of Engineering Materials and Technology*, (115), pp.417-423, 1993.

[6] Y. UEDA, H. MURAKAWA, N.X. MA: 'Measuring Method for Residual Stresses in Explosively Clad Plates and a Method of Residual Stress Reduction', *Journal of Engineering Materials and Technology*, (118), pp.76-582, 1996.

[7] V. PLOSHIKHIN, A. PRIHODOVSKY, A. ILIN, C. HEIERDINGER: 'Advanced numerical method for fast prediction of welding distortions in large aircraft structures', *International Journal of Microstructure and Materials Properties*, (5), pp.423-435, 2010.

[8] V. PLOSHIKHIN, A. PRIHODOVSKY, T. FRANK, A. ILIN, D. BÄCHLE, P. KRAFT, C. HEIMERDINGER: 'Schweißverzüge bei Großbauteilen verstehen und beherrschen', *Tagungsband Große Schweißtechnische Tagung, DVS-Berichte Band 250*, pp.338-340, 2008.

[9] V. PLOSHIKHIN, A. PRIHODOVSKY, T. FRANK, A. ILIN, C. HEIMERDINGER: 'Advanced numerical method for fast prediction of welding distortions of large aircraft structures', *Proc. 2nd International Conference Distortion Engineering IDE*, 491-498, 2008.

[10] V. PLOSHIKHIN, A. PRIHODOVSKY, A. ILIN, C. HEIMERDINGER, F. PALM: 'Beherrschung der Schweißverzüge bei Großbauteilen', *Tagungsband Große Schweißtechnische Tagung, DVS-Berichte Band 258*, pp.104-107, 2009.

[11] V. PLOSHIKHIN, A. PRIHODOVSKY, A. ILIN, C. HEIMERDINGER: 'Advanced numerical method for fast prediction of welding distortions in large aircraft structures', *International Journal of Microstructure and Materials Properties*, Vol. 5, Nos. 4/5, pp. 423-435, 20010.

[12] A. PRIHODOVSKY, V. PLOSHIKHIN, A. ILIN, R. LOGVINOV, C. HEIMERDINGER, F. PALM: 'Efficient numerical method for the prediction of welding distortions and its application to large aircraft structures', *Mathematical Modelling of Weld Phenomena 9*, Verlag der Technischen Universität Graz, pp. 493-522, 2010

[13] A. ILIN: *Methode zur effizienten FEM-Simulation der schweißprozessbedingten Deformationen von Großbauteilen*, thesis, University of Bremen, 2013.

[14] M.SCHAENZEL, D.SHAKIROV, A. ILIN, V. PLOSHIKHIN: 'Coupled thermo-mechanical process simulation method for selective laser melting considering phase transformation steels, *International Journal of Computers & Mathematics with Applications*, to be published in 2018.

[15] J. GOLDAK, A. CHAKRAVARTI, M. BIBBY: 'A new finite element model for welding heat sources', *Metallurgical Trans. B 15B*, pp. 299-305, 1984

[16] D. KOISTINEN, R. MARBURGER: 'A general equation prescribing the extent of the austenite-martensite transforamtion in pure iron-carbon alloys and plain carbon steels', *Acta Metallurgica 7*, 1958

[17] N. SAUNDERS, U.K.Z. GUO, X. LI ET AL.: 'JOM 55: 60', *[Online] Available at: www.doi.org/10.1007/s11837-003-0013-2*, 2003

[18] DÖRRENBERG EDELSTAHL GMBH: 'Material data sheet 1.4057 X17CrNi16-2', *[Online] Available at: www.doerrenberg.de/uploads/tx_c1x1downloads/1.4057_de_01.pdf*, 2018
[19] SIMULIA: *Abaqus analysis User's Manual*, *2017*, Providence, Rhode Island, 2017
[20] E. KARDOULAKI, J. LIN, D. BALINT, D. FARRUGIA: 'Investigation of the effects of thermal gradients present in Gleeble high-temperature tensile tests on the strain state for free cutting steel', *The Journal of Strain Analysis for Engineering Design* ,Vol. 49, 2014
[21] K. SATOH: 'Transient Thermal Stresses of Weld Heat-Affected Zone by Both Ends Fixed Analogy', *Transaction of the Japan Welding Society* ,Vol. 3, No.1, 1972